Supporting Information

# Exposing the abundant active sites in amorphous NiCuFeP@$Cu_3P$ branch-like nanoarrays for efficient electrocatalytic hydrogen evolution reaction

Jiaxing Jin, Jingmin Ge, Xuhui Zhao, Yiping Wang*, Fazhi Zhang, Xiaodong Lei*

State Key Laboratory of Chemical Resource Engineering, Beijing University of Chemical Technology, PO Box 98, Beijing 100029, China.

Tel: +86-10-64455357; Fax: +86-10-64425385

* Corresponding author

E-mail: wangyiping@buct.edu.cn (Yiping Wang)

leixd@mail.buct.edu.cn (Xiaodong Lei)

**Content** Figures (on page S3-S10), Tables (on page S11-S12), References (on page S15-S-18)

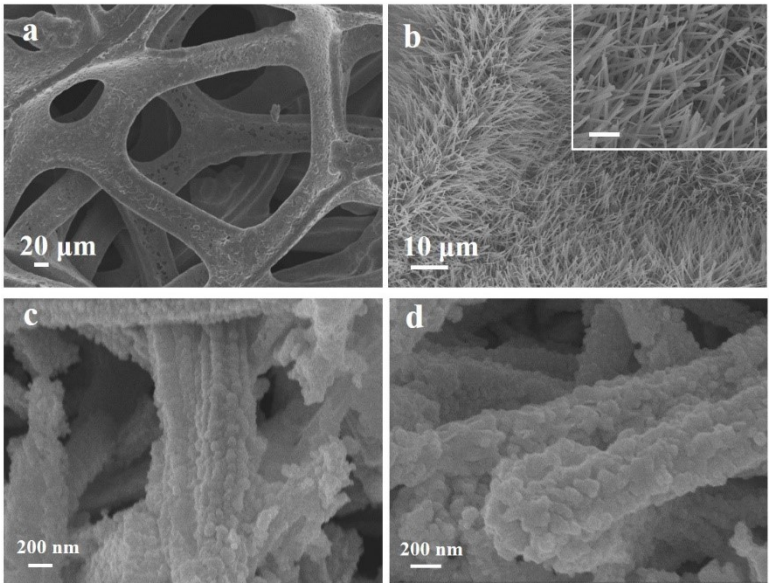


**Fig. S1** SEM images of Cu Foam (a), $Cu(OH)_2$/CF (b) (inset: partial magnification of $Cu(OH)_2$ nanowires), NiP@$Cu_3P$/CF (c) and NiFeP@$Cu_3P$/CF (d).

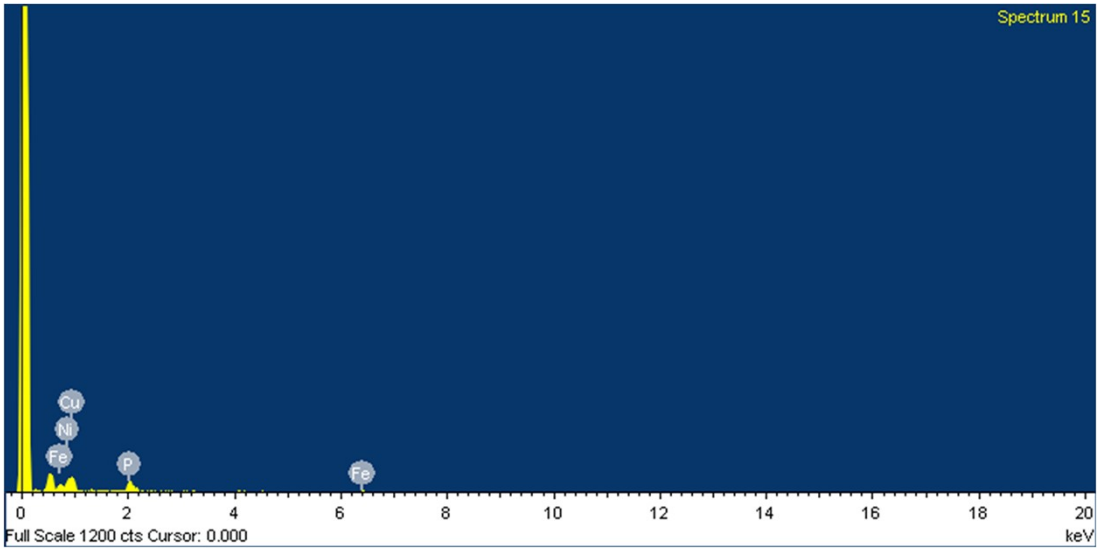


**Fig. S2** EDS of NiCuFeP@$Cu_3P$/CF

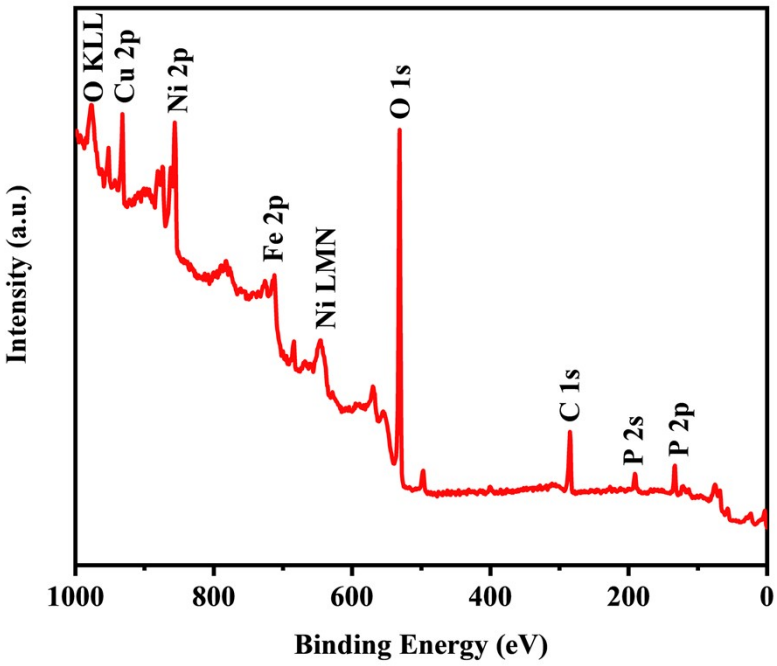


**Fig. S3** XPS survey of NiCuFeP@$Cu_3P$/CF.

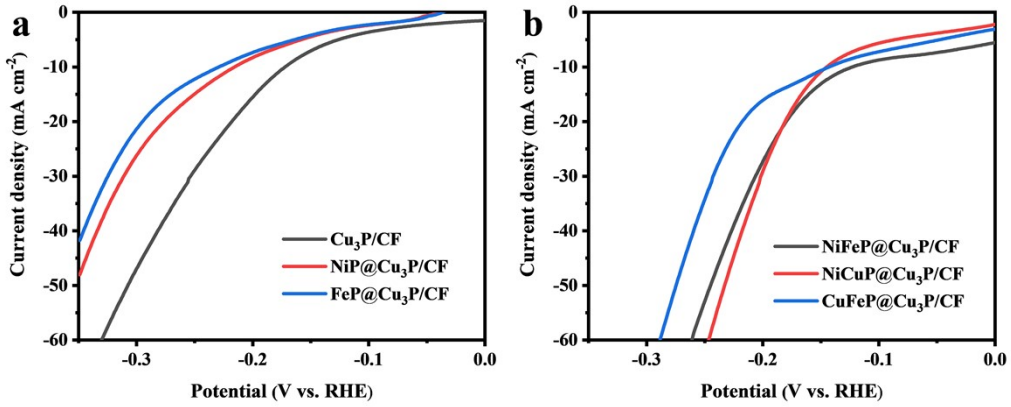


**Fig. S4** LSV curves of (a) $Cu_3P$/CF, NiP@$Cu_3P$/CF and FeP@$Cu_3P$/CF, (b) NiFeP@$Cu_3P$/CF, NiCuFeP@$Cu_3P$/CF and CuFeP@$Cu_3P$/CF.

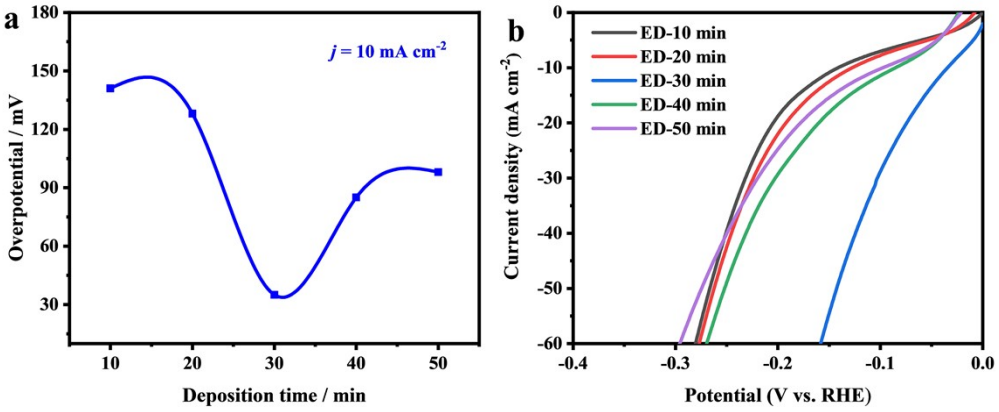


**Fig. S5** Overpotential (a) and LSV curves (b) of different deposition time for NiCuFeP@$Cu_3P$/CF.

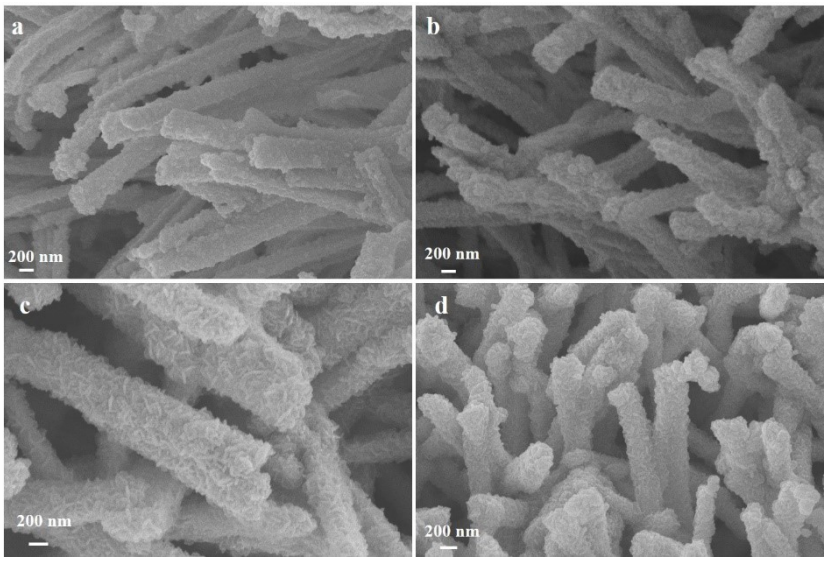


**Fig. S6** SEM images of different deposition times (a) 10, (b) 20, (c) 40 and (d) 50 min.

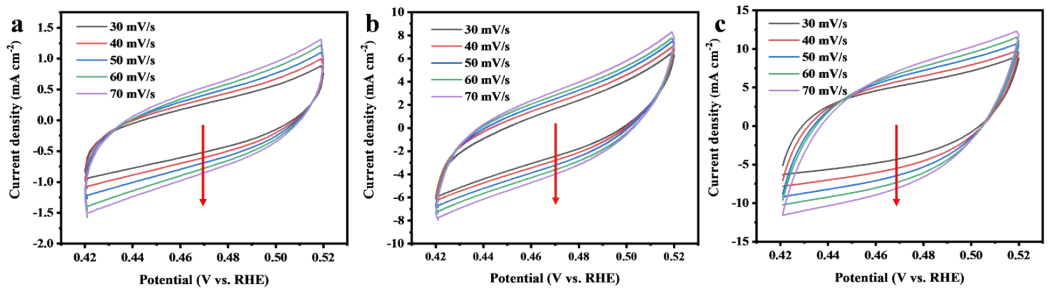


**Fig. S7** Cyclic voltammograms of Cu Foam (a), $Cu_3P$/CF (b) and NiCuFeP@$Cu_3P$/CF (c).

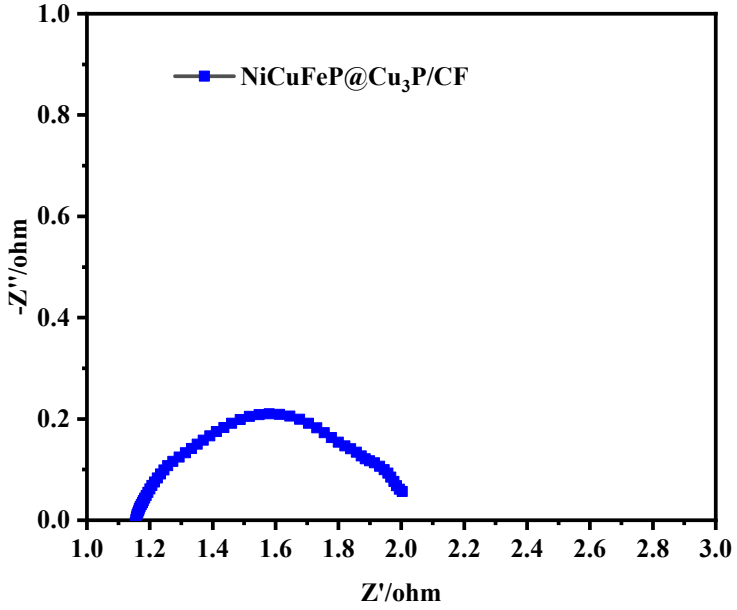


**Fig. S8** Nernst plots of NiCuFeP@$Cu_3P$/CF with small coordinate range.

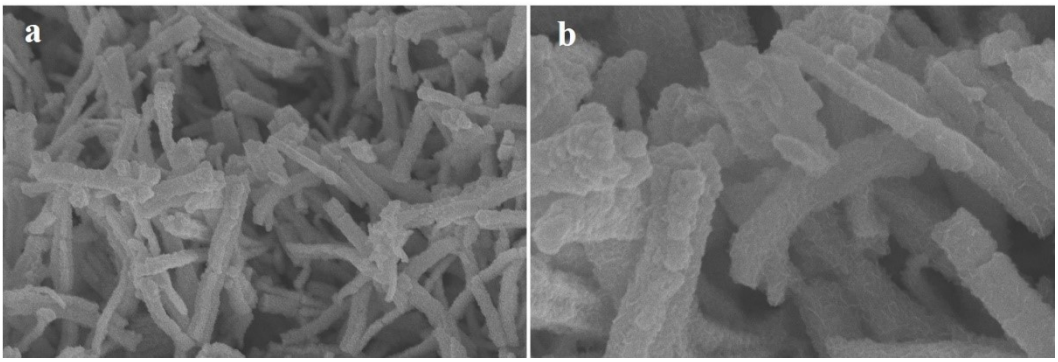


**Fig. S9** SEM images of NiCuFeP@$Cu_3P$/CF after 20 h i-t stability test.

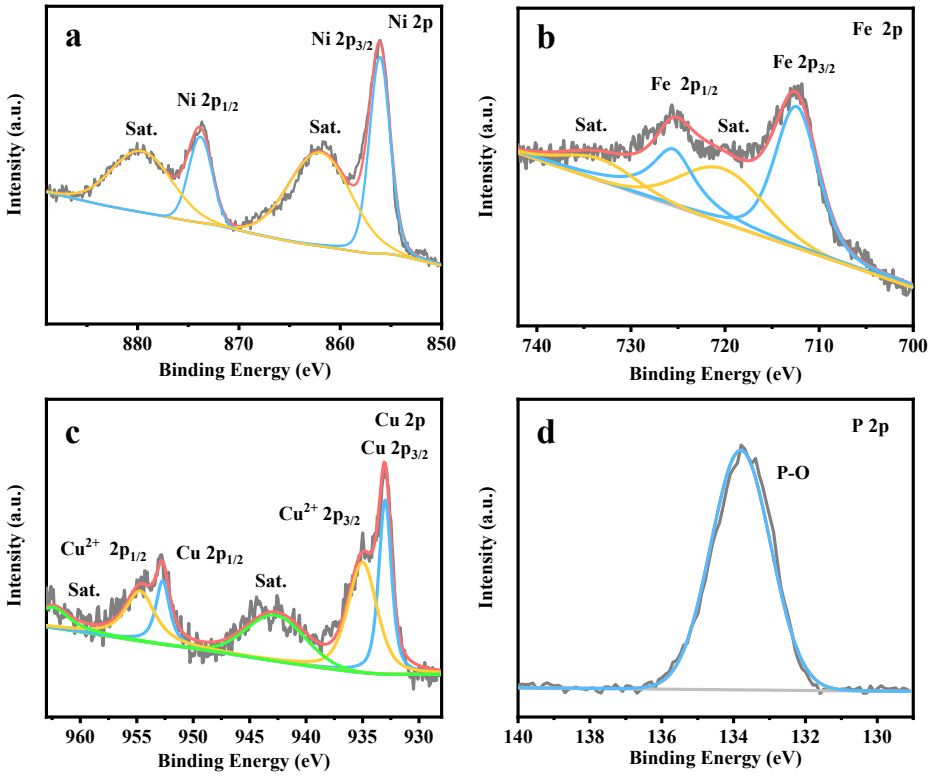


**Fig. S10** XPS of NiCuFeP@Cu3P/CF after the HER test for (a) Ni 2p, (b) Fe 2p, (c) Cu 2p and (d) P 2p.

**Table S1.** Comparison with some recently reported nonprecious HER electrocatalysts measured in 1.0 M KOH.

| Catalyst | Overpotential vs. RHE (mV) | Tafel slope mV/dec | Current density (mA $cm^{-2}$) | Reference |
|---|---|---|---|---|
| NiCuFeP@$Cu_3P$/CF | 38 | 96.8 | 10 | This work |
| PSS-PPy/Ni-Co-P/CF | 64 | 27.38 | 10 | [1] |
| CoP/$Ni_2P$@HPNCP | 106 | 61.89 | 10 | [2] |
| $NC_{0.9}F_{0.1}P$ HHAs/NF | 122.5 | 54.36 | 10 | [3] |
| g-$FeO_x$–$Cu_3P$@Cu | 48 | 58.80 | 10 | [4] |
| $NiCu_{0.05}Fe_{0.025}$ PNW | 64 | 60.80 | 10 | [5] |
| NiCoP@$Cu_3P$/Cu | 54 | 72 | 10 | [6] |
| $Cu_3P$-$Ni_2P$/NF | 103 | 80 | 10 | [7] |
| $Ni_2P$-$Cu_3P$@NiCuC | 78 | 173 | 10 | [8] |
| H-MoS/MoP | 92 | 59.80 | 10 | [9] |
| NiFeP-$MoO_2$/NF | 56 | 80.5 | 10 | [10] |
| NiFeP@N-CS | 186 | 112 | 10 | [11] |
| FeP/HCNB | 180 | 71 | 10 | [12] |
| NPC $FeP_{30min}$/ CP | 140 | 61.92 | 10 | [13] |
| 3D FeP NS | 116 | 57 | 10 | [14] |
| Ni–P/$Ni(OH)_2$ NTs | 54.7 | 58 | 10 | [15] |
| CoP@a-CoB HNRA | 56.3 | 62.0 | 10 | [16] |
| FF–NaCl–Ir–P | 69 | 87.8 | 10 | [17] |
| MoP/NiFeP HS | 73 | 31 | 10 | [18] |
| NiO@NiP/NF | 76 | 98 | 10 | [19] |
| S-NiCoP NW/CFP | 102 | 63.3 | 10 | [20] |

**Table S2.** Resistance of the Cu Foam, $Cu_3P$/CF and NiCuFeP@$Cu_3P$/CF materials.

| | Cu Foam | $Cu_3P$/CF | NiCuFeP@$Cu_3P$/CF |
|---|---|---|---|
| **$R_s$** | 1.497 | 1.96 | 1.148 |
| **CPE-T** | 0.007 | 0.123 | 0.108 |
| **CPE-P** | 0.870 | 0.702 | 0.594 |
| **$R_{ct}$** | 23.87 | 10.79 | 0.833 |

**References**


1 F. Tian, S. Geng, L. He, Y. Huang, A. Fauzi, W. Yang, Y. Liu and Y. Yu, Interface engineering: PSS-PPy wrapping amorphous Ni-Co-P for enhancing neutral-pH hydrogen evolution reaction performance, *Chem. Eng. J.*, 2021, 417, 129232.

2 R. Zhang, R. Zhu, Y. Li, Z. Hui, Y. Song, Y. Cheng and J. Lu, CoP and $Ni_2P$ implanted in a hollow porous N-doped carbon polyhedron for pH universal hydrogen evolution reaction and alkaline overall water splitting, *Nanoscale*, 2020, 12, 23851-23858.

3 Y. Qi, Q. Zhang, S. Meng, D. Li, W. Wei, D. Jiang and M. Chen, Iron-doped nickle cobalt ternary phosphide hyperbranched hierarchical arrays for efficient overall water splitting, *Electrochim. Acta*, 2020, 334, 135633.

4 C. Tong, R. Xiang, L. Peng, L. Tan, X. Tang, J. Wang, L. Li, Q. Liao and Z. Wei, Amorphous $FeO_x$ (x = 1, 1.5) coated $Cu_3P$ nanosheets with bamboo leaves-like morphology induced by solvent molecule adsorption for highly active HER catalysts, *J. Mater. Chem. A*, 2020, 8, 3351-3356.

5 C. Hegde, X. Sun, K. N. Dinh, A. Huang, H. Ren, B. Li, R. Dangol, C. Liu, Z. Wang, Q. Yan and H. Li, Cu- and Fe-Codoped Ni Porous Networks as an Active Electrocatalyst for Hydrogen Evolution in Alkaline Medium, *ACS Appl. Mater. Interfaces*, 2020, 12, 2380-2389.

6 X. Ma, Y. Chang, Z. Zhang and J. Tang, Forest-like NiCoP@$Cu_3P$ supported on copper foam as a bifunctional catalyst for efficient water splitting, *J. Mater.*

*Chem. A*, 2018, 6, 2100-2106.

7 X. Jin, J. Li, Y. Cui, X. Liu, X. Zhang, J. Yao and B. Liu, $Cu_3P$-$Ni_2P$ Hybrid Hexagonal Nanosheet Arrays for Efficient Hydrogen Evolution Reaction in Alkaline Solution, *Inorg Chem*, 2019, 58, 11630-11635.

8 L. Yu, J. Zhang, Y. Dang, J. He, Z. Tobin, P. Kerns, Y. Dou, Y. Jiang, Y. He and S. L. Suib, In Situ Growth of $Ni_2P$–$Cu_3P$ Bimetallic Phosphide with Bicontinuous Structure on Self-Supported NiCuC Substrate as an Efficient Hydrogen Evolution Reaction Electrocatalyst, *ACS Catal.*, 2019, 9, 6919-6928.

9 Q. Liu, Z. Xue, B. Jia, Q. Liu, K. Liu, Y. Lin, M. Liu, Y. Li and G. Li, Hierarchical Nanorods of $MoS_2$/MoP Heterojunction for Efficient Electrocatalytic Hydrogen Evolution Reaction, *Small*, 2020, 16, e2002482.

10 X. Wu, J. Li, Y. Li and Z. Wen, NiFeP-$MoO_2$ hybrid nanorods on nickel foam as high-activity and high-stability electrode for overall water splitting, *Chem. Eng. J.*, 2021, 409, 128161.

11 J. Hei, G. Xu, B. Wei, L. Zhang, H. Ding and D. Liu, NiFeP nanosheets on N-doped carbon sponge as a hierarchically structured bifunctional electrocatalyst for efficient overall water splitting, *Appl. Surf. Sci.*, 2021, 549, 149297.

12 Z. Peng, X. Qiu, Y. Yu, D. Jiang, H. Wang, G. Cai, X. Zhang and Z. Dong, Polydopamine coated prussian blue analogue derived hollow carbon nanoboxes with FeP encapsulated for hydrogen evolution, *Carbon*, 2019, 152, 16-23.

13 J. Shi, F. Qiu, W. Yuan, M. Guo, C. Yuan and Z.-H. Lu, Novel electrocatalyst of nanoporous FeP cubes prepared by fast electrodeposition coupling with acid-

etching for efficient hydrogen evolution, *Electrochim. Acta*, 2020, 329, 135185.

14 M. Guo, Y. Qu, C. Yuan and S. Chen, Electrochemically assisted synthesis of three-dimensional FeP nanosheets to achieve high electrocatalytic activity for hydrogen evolution reaction, *Int. J. Hydrogen Energy*, 2019, 44, 24197-24208.

15 F. Zhao, H. Liu, H. Zhu, X. Jiang, L. Zhu, W. Li and H. Chen, Amorphous/amorphous Ni–P/$Ni(OH)_2$ heterostructure nanotubes for an efficient alkaline hydrogen evolution reaction, *J. Mater. Chem. A*, 2021, 9, 10169-10179.

16 P. Shi, Y. Zhang, G. Zhang, X. Zhu, S. Wang and A.-L. Wang, A crystalline/amorphous CoP@CoB hierarchical core–shell nanorod array for enhanced hydrogen evolution, *J. Mater. Chem. A*, 2021, 9, 19719-19724.

17 Z. Zhao, W. Jin, L. Xu, C. Wang, Y. Zhang and Z. Wu, Ultrafine Ir nanoparticles decorated on FeP/FeOOH with abundant interfaces via a facile corrosive approach for alkaline water-splitting, *J. Mater. Chem. A*, 2021, 9, 12074-12079.

18 L. Lin, M. Chen and L. Wu, Hierarchical MoP/NiFeP hybrid hollow spheres as highly efficient bifunctional electrocatalysts for overall water splitting, *Mater. Chem. Front.*, 2021, 5, 375-385.

19 C. Sun, H. Wang, J. Ren, X. Wang and R. Wang, Inserting ultrafine NiO nanoparticles into amorphous NiP sheets by in situ phase reconstruction for high-stability of the HER catalysts, *Nanoscale*, 2021, 13, 13703-13708.

20 Y. Qi, L. Zhang, L. Sun, G. Chen, Q. Luo, H. Xin, J. Peng, Y. Li and F. Ma, Sulfur doping enhanced desorption of intermediates on NiCoP for efficient

alkaline hydrogen evolution, *Nanoscale*, 2020, 12, 1985-1993.